Supplemental Methods

Flow cytometry

Peritoneal exudates were stained with anti-F4/80-APC (BM8; eBioscience), -CD11b-PE-Cy7 (M1/70; BioLegend), -I-A^b-FITC (116406; BioLegend) and -CD40-PE (3/23; BD Pharmingen) and analyzed on a Gallios cytometer (Beckman Coulter). The data were analyzed with FlowJo software (Tristar).

Spleens were isolated at 2 h post-LPS rechallenge, and a single-cell suspension was made by passing a spleen through a 40 μm cell strainer (BD Falcon). After red cell lysis by ammonium chloride solution and Fc receptor blocking (1 μl of Fc-receptor blocking antibody for 15 min at 4°C; 082832121; Beckman Coulter), splenocytes were stained with anti-CD19-APC (6D5; Southern), -CD25-PeCy7 (PC61; BioLegend), -CD86-PE (GL-1; BioLegend), -I-A^b-FITC (116406; BioLegend) for B cell analysis; anti-CD4-PeCy7 (GK1.5; BioLegend), -CD8-PerCP (53-6.7; BioLegend), -CD69-PE (H1.2F3; BD Pharmingen) for T cell analysis; -F4/80-APC (BM8; eBioscience), -CD11b-PeCy7 (M1/70; BioLegend), -I-A^b-FITC (116406; BioLegend), -CD40-PE (3/23; BD Pharmingen) for macrophage analysis; anti-CD11c-APC (N418; eBioscience), -CD19-SPRD (6D5; Southern), -B220-PeCy7 (RA3-6B2; BioLegend), -CD69-PE (H1.2F3; BD Pharmingen), -I-A^b-FITC (116406; BioLegend) for dendritic cell analysis.

Endothelial cell isolation and culture

Lung endothelial cells were isolated as previously described (81). Lungs were excised from ketamine (100 mg/kg; i.p.) and xylazine (10 mg/kg; i.p.) anasthetized WT and $p21^{-/-}$ mice, cut in pieces and digested with collagenase/dispase solution. After dispersion as a single-cell suspension, endothelial cells were purified using positive selection with anti-PECAM-1 (CD-31) antibody (Clone 390; BD Pharmingen) conjugated to dynabeads (Invitrogen); >90% of the isolated cells were CD-31^+, as

determined by flow cytometry, using anti-CD31-PE (MEC 13.3, BD Biosciences). Purified cells were plated onto gelatin-coated tissue culture plates and cultured in VascuLife with EnGS-Mv Life Factors Kit (Lifeline Cell Technology) and penicillin/streptomycin. When cells reached confluence (after 5 days) they were plated in 6-well plates at a density of 0.3×10^6 cells/well. Six days later, endothelial cells were subjected to two consecutive LPS treatments to induce tolerance, as described for peritoneal macrophages.

Cell cycle analysis

To analyze cell cycle, 1×10^6 cells were permeabilized with detergent, stained with PI according to the manufacturer's instructions (DNA-Prep Reagent Kit, Beckman Coulter) for 30 min at 37°C, and analyzed by flow cytometry.

CDK2 kinase assay

For CDK2 kinase assay, cells were lysed in buffer containing 50 mM Tris-HCl (pH 7.5), 150 mM NaCl, 0.5% NP-40, protease inhibitor cocktail and phosphatase inhibitor cocktail (Roche). Protein lysates (200 μg) were mixed overnight at 4° C with 2 μg anti-CDK2 (M2, Santa Cruz) and incubated with pre-blocked protein G-Sepharose beads (25 μl, Invitrogen) for additional 2 h. Anti-CDK2 immunoprecipitates were then incubated with 20 μl kinase buffer (20 mM Tric-HCl (pH 8.0), 10 mM $MgCl_2$, 1 mM EGTA, 1 mM dithiothreitol, 1 mM NaF, protease inhibitor cocktail and phosphatase inhibitor cocktail), supplemented with 5 μg histone H1 (Roche), 0.5 mM ATP (Cell Signaling) and 10 μCi [γ-^{32}P]ATP (3000 Ci/mmol; Perkin Elmer; 30 min at 30° C). Phosphorylated histone H1 was resolved by gel electrophoresis.

Real-Time PCR

Macrophage cultures were washed with ice-cold PBS and total RNA was extracted with TRIzol (Sigma) according to the manufacturer's instructions. Reverse transcription

from 1 μg of RNA was performed using the cDNA kit (Appled Biosystems). Real-time PCR was performed using EvaGreen Master Mix (Solis BioDyne) and detected by the ABI PRISM 7900HT (Applied Biosystems). Data were processed using SDS 2.4 software (Applied Biosystems). Results were normalized to the expression of the β-actin and presented as the fold induction with respect to the control cell population. Due to high IL-10 mRNA levels in unstimulated cells, results of IL-10 expression were normalized to unstimulated cells of each genotype to calculate the amplitude of the transcription response ("dynamic range") (73) after stimulation. The products were amplified using primers for p21, 5'-GCA GAT CCA CAG CGA TAT CC-3' (forward) and 5'-CAA CTG CTC ACT GTC CAC GG-3' (reverse); arginase I, 5'-CAC TCC CCT GAC AAC CAG CT-3' (forward) and 5'-AAG GAC ACA GGT TGC CCA TG-3' (reverse); YM1, 5'-ACT TTG ATG GCC TCA ACC TG-3' (forward) and 5'-AAT GAT TCC TGC TCC TGT GG-3' (reverse); CCL17, 5'-GGC CTT GGG TTT TCA CCA-3' (forward) and 5'-CAG GGA TGC CAT CGT GTT TC-3' (reverse); CCL22, 5'-CCT GGG ATC GGC ACA GAT A-3' (forward) and 5'-CAC CCT CTG CCA TCA CGT TT-3' (reverse); TNF-α 5'-CTG TAG CCC ACG TCG TAG C-3' (forward) and 5'-TTG AGA TCC ATG CCG TTG-3' (reverse); IL-1β, 5'-TGG TGT GTG ACG TTC CCA TT-3' (forward) and 5'-CAG CAC GAG GCT TTT TTG TTG-3' (reverse); IFN-β, 5'-TCA GAA TGA GTG GTG GTT GC-3' (forward) and 5'-GAC CTT TCA AAT GCA GTA GAT TCA-3' (reverse); iNOS, 5'-GCT GTG CTC CAT AGT TTC CAG-3' (forward) and 5'-GGA CCA GCC AAA TCC AGT C-3' (reverse); CXCL11, 5'-AAA GAC AGC GCC CCT-3' (forward) and 5'-GGC TGC TGA GAT GAA CAG GAA-3' (reverse); IL-10, 5'-CGG GAA GAC AAT AAC TG-3' (forward) and 5'-CAT TTC CGA TAA GGC TTG G-3' (reverse); IRAK-M, 5'-TGA GCA ACG GGA CGC TTT-3' (forward) and 5'-GAT TCG AAC GTG CCA GGA A-3' (reverse); p105, 5'-CAT

GGC AGA CGA TGA TCC C-3' (forward) and 5'-ATT TGA AGG TAT GGG CCA T-3' (reverse); Bcl-3, 5'-CCT TTG ATG CCC ATT TAC TC-3' (forward) and 5'-AGC GGC TAT GTT ATT CTG G-3' (reverse); β-actin, 5'-GGC TGT ATT CCC CTC CAT CG-3' (forward) and 5'-CCA GTT GGT AAC AAT GCC ATG T-3' (reverse). All primers were synthesized, desalted, and purified by Sigma.

For human samples, RNA was isolated using the High Pure RNA Isolation Kit (Roche Diagnostics). The cDNA was obtained by reverse transcription of 1μg RNA using the High Capacity cDNA Reverse Transcription Kit (Applied Biosystems). Real-time quantitative PCR was performed using the QuantiMix Easy SYG kit from Biotools. Results were normalized to the expression of β-actin, and the cDNA copy number for each gene was determined using a 7-point standard curve, as described previously (82). The products were amplified using primers for TNF-α, 5'-GCC TCT TCT CCT TCC TGA TCG T-3' (forward) and 5'-CTC GGC AAA GTC GAG ATA GTC G-3' (reverse); CCL2, 5'-GAT CTC AGT GCA GAG GCT CG-3' (forward) and 5'-ATT CTT GGG TTG TGG AGT GAG TGT TCA-3' (reverse); p21, 5'-GAG GCC GGG ATG AGT TGG GAG GAG-3' (forward) and 5'-CAG CCG GCG TTT GGA GTG GTA GAA-3' (reverse); IFN-β, 5'-CCT GGC TAA TGT CTA TCA TCA-3' (forward) and 5'-GCA GTA CAT TAG CCA TCA GTC-3' (reverse); β-actin, 5'-AAG AGC TAC GAG CTG CCT GAC G-3' (forward) and 5'-TCC ACA TCT GCT GGA AGG TGG-3' (reverse). The primers were synthesized, desalted and purified by Bonsai Biotech.

Western blot

To obtain whole cell extracts, macrophage cultures were washed with ice-cold PBS and lysed in a buffer containing 0.2% Nonidet P-40, 10 mM Tris-HCl [pH 7.5], 150 mM NaCl, and 1 × protease and phosphatase inhibitor cocktail (Roche), for 20 min at 4°C. Nuclear extracts were separated from cytoplasmic fraction using Nuclear/Cytosol

Fractination Kit (Bio Vision). The lysates were centrifuged at 14,000 × *g* for 15 min; the supernatants were measured using the Bio-Rad protein assay and resolved in 12% SDS-PAGE (20 μg protein per lane). Proteins were next transferred into a nitrocellulose membrane (75 min at 300 mA) and immunoblotted using antibodies against p21 (C-19), p50 (E-10), p65 (sc-109), CDK2 (M2), Bcl-3 (C-14), (Santa Cruz Biotechnology), phospho-STAT1 (Y701), phospho ERK (#9106), IκBα (#9242), phospho IRF3 (#4947) (Cell Signaling), iNOS (ab15323), histone H1 (ab71580) (Abcam), JNK (44682G; Invitrogen), actin (AC-15; Sigma). HRP-conjugated secondary antibodies (Dako) were used at dilution of 1:2,000 for 1 h at room temperature. Blots were visualized using Western Lightning Plus-ECL (PerkinElmer).

EMSA

NF-κB double stranded consensus oligonucleotides (5'-AGT TGA GGG GAC TTT CCC AGG C-3') were purchased from Promega; double stranded oligonucleotides corresponding to the PRDII domain of the IFN-β promoter (5'-GGG AAA TTC CGG GAA ATT CC-3') and oligonucleotides with mutant NF-κB sites (5'-act AAA TTC CAC TAA ATT CC-3') were purchased from Sigma. They were end-labeled with [γ^{32}P]ATP (PerkinElmer) using the T4 polynucleotide kinase (Promega). Binding reactions were prepared using 5 μg of nuclear extract in a 25 μl reaction volume containing 0.5 ng labeled oligonucleotide probe, 10 mM HEPES, 1 mM $MgCl_2$, 35 mM NaCl, 0.5 mM EDTA, 0.5 mM DTT, 10% glycerol, 1 μg bovine serum albumin and 1.5 μg poly[d(I-C)] at room temperature for 30 min.

Small interfering RNA

p21 (ID 1531) and the control small interfering RNAs (siRNAs) were designed and synthesized by Life Technologies. Human monocytes were transfected with siRNAs using the Amaxa Nucleofector system (Amaxa Biosystems). Briefly, 1.5 × 10^6

monocytes were nucleofected with 30 μM siRNA mixed with 100 μl nucleofection solution, according to the manufactrer's instructions. The cells were then immediately transferred to a six-well culture plate (Costair) in a final volume of 2 ml prewarmed RPMI 1640 media supplemented with 10% heat-inactivated FBS (Invitrogen). The nucleofected cells were cultured at 37°C with 5% CO_2 for 1 h before the assays.

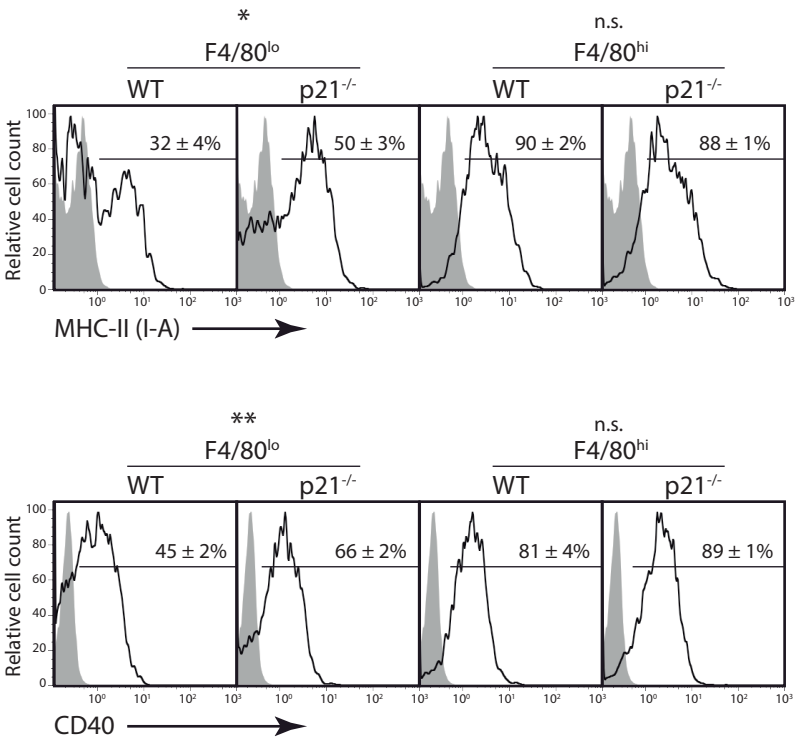

Figure S1. p21 limits activation of F4/80^{lo} but not F4/80^{hi} peritoneal macrophages during *in vivo* endotoxin tolerance. p21$^{-/-}$ and WT mice received two LPS doses as in Figure 1. At 2 h after the second injection, peritoneal exudate was harvested and macrophage populations analyzed by flow cytometry. CD11b^{hi}F4/80^{lo} cells from p21$^{-/-}$ mice showed increased MHC Class II and CD40 surface expression compared with WT; expression of these activation markers was similar in CD11b^{hi}F4/80^{hi} cells in both mouse strains. Data show mean ± SEM, $n = 3$ mice, *$p<0.05$, **$p<0.001$, n.s., not significant; two-tailed Student's *t* test.

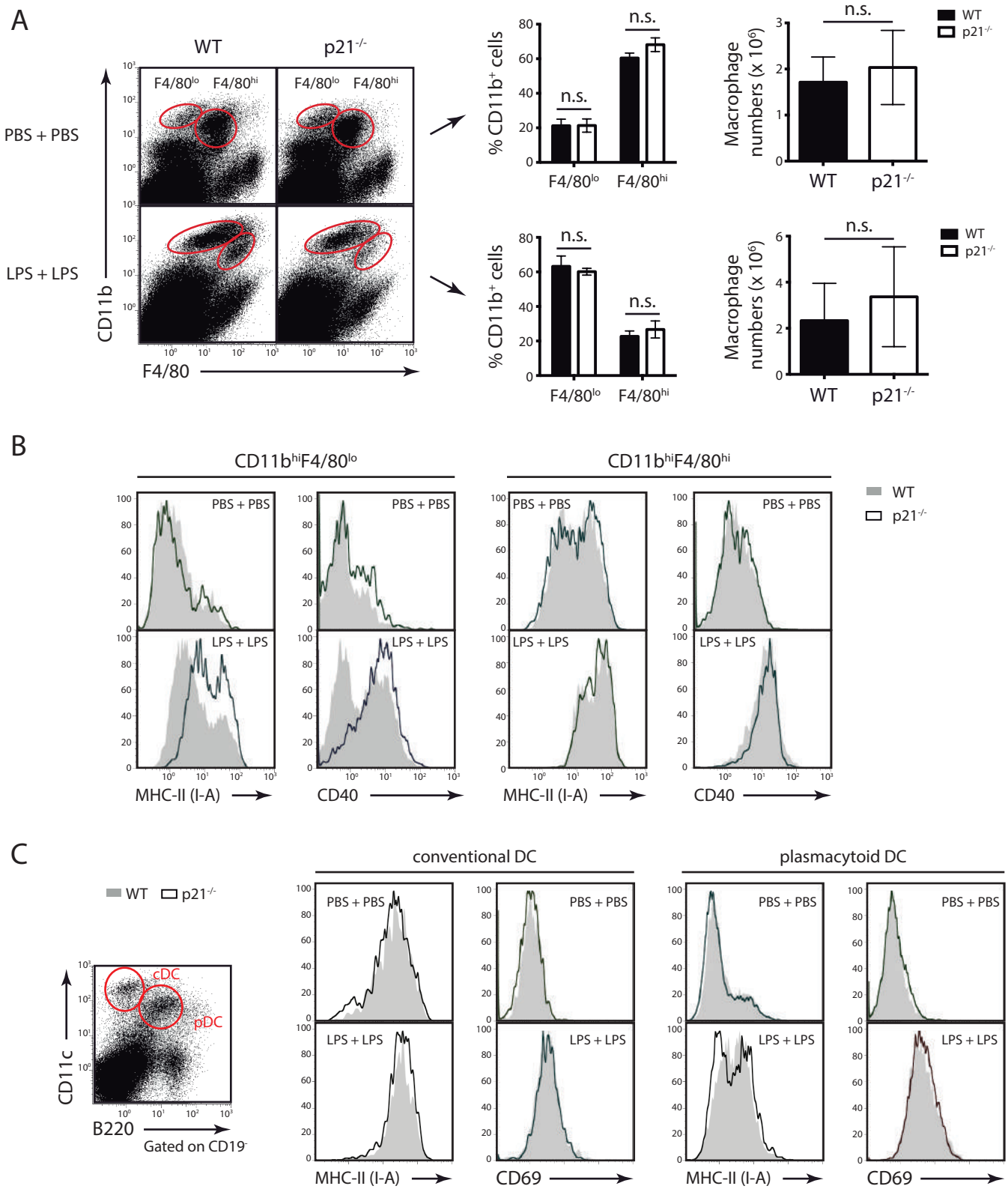

Figure S2. p21 does not affect activation of spleen macrophages and dendritic cells during *in vivo* endotoxin tolerance. p21$^{-/-}$ and WT mice received two LPS doses as in Figure 1. At 2 h after the second injection, total splenocytes were analyzed by flow cytometry. (**A**) Representative plots show gated CD11b^{hi}F4/80^{lo} and CD11b^{hi}F4/80^{hi} macrophage populations. The relative percentages of these two populations within the total CD11b^{+} gate, as well as total macrophage numbers, were similar for WT and p21$^{-/-}$ mice after dual LPS or PBS treatment. Data show mean ± SD (n = 6 mice); n.s., not significant; two-tailed Student's t test. (**B**) Representative histograms (n = 3 mice) showing increased MHC Class II and CD40 surface expression in CD11b^{hi}F4/80^{lo} cells from p21$^{-/-}$ compared with WT mice; expression of these activation markers was similar in CD11b^{hi}F4/80^{hi} cells in both mouse strains. (**C**) Staining profile of CD19^{-} splenocytes showing two dendritic cell subsets, CD11c^{hi}B220^{-} conventional dendritic cells (cDC) and CD11c^{int}B220^{+} plasmacytoid dendritic cells (pDC). Both DC subsets showed similar activation in WT and p21$^{-/-}$ mice, as seen by surface expression of MHC Class II and CD69. Representative histograms are shown (n = 3 mice).

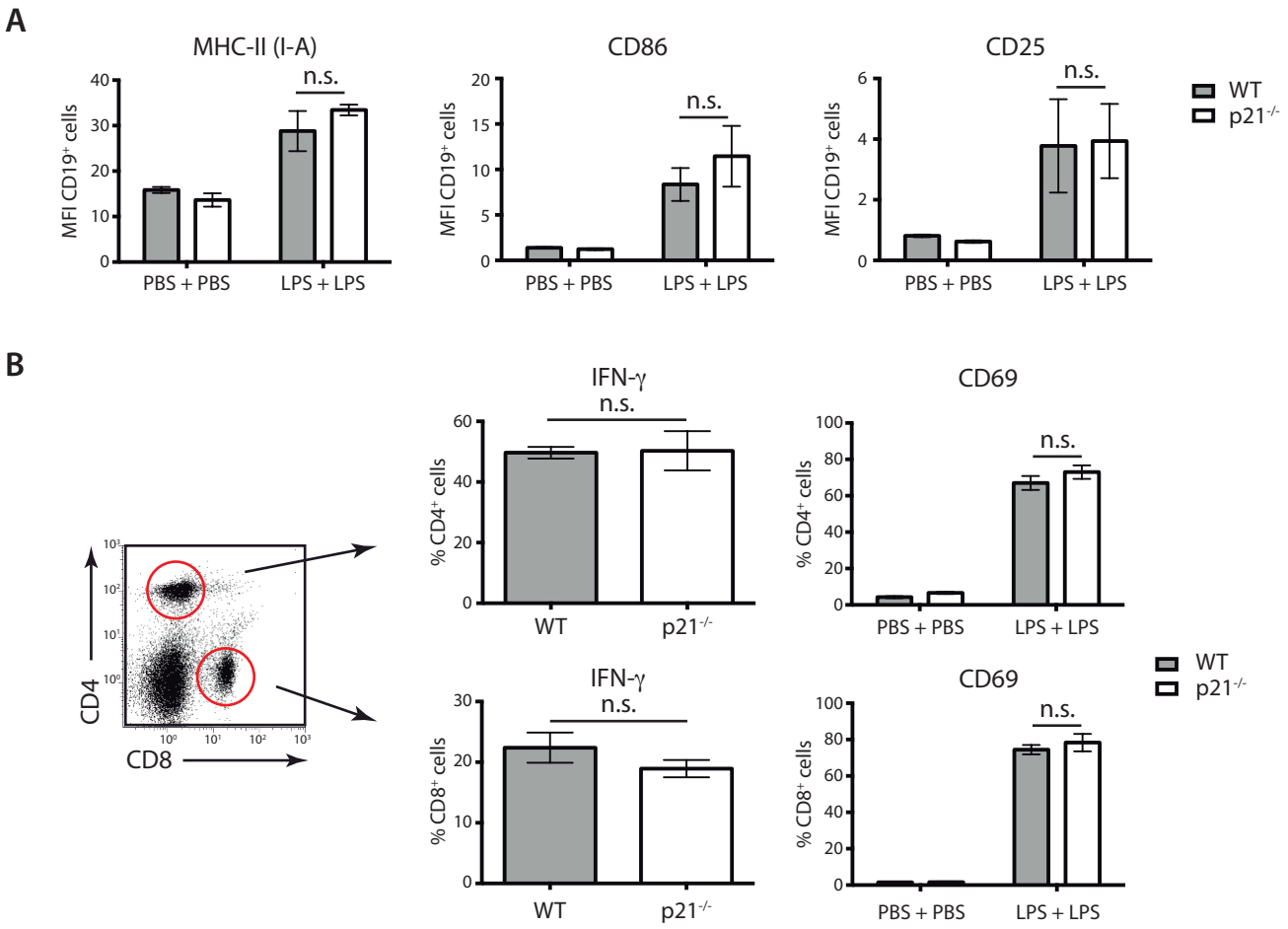

Figure S3. p21 does not affect B and T cell activation during *in vivo* endotoxin tolerance. p21$^{-/-}$ and WT mice received two LPS doses as in Figure 1. At 2 h after the second injection, total splenocytes were analyzed by flow cytometry. (**A**) Similar frequencies of CD19^{+} B cells expressing MHC Class II, CD86 and CD25 activation markers in WT and p21$^{-/-}$ mice. (**B**) Similar frequencies of IFN-γ-producing and CD69-expressing CD4^{+} (top) and CD8^{+} (bottom) T cells in WT and p21$^{-/-}$ mice. Data show mean ± SEM (n = 3 mice); n.s., not significant; two-tailed Student's t test.

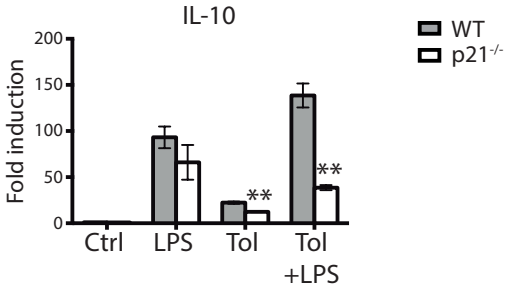

Figure S4. IL-10 expression in tolerized peritoneal macrophages. Peritoneal macrophages from WT and p21$^{-/-}$ mice were treated as in Figure 3. After LPS tolerization, p21$^{-/-}$ macrophages showed decreased IL-10 induction compared with WT macrophages. Results were normalized to β-actin and represent fold induction over unstimulated cells of each genotype. Data show mean ± SEM (n = 3); ** p<0.01, two-tailed Student's t test.

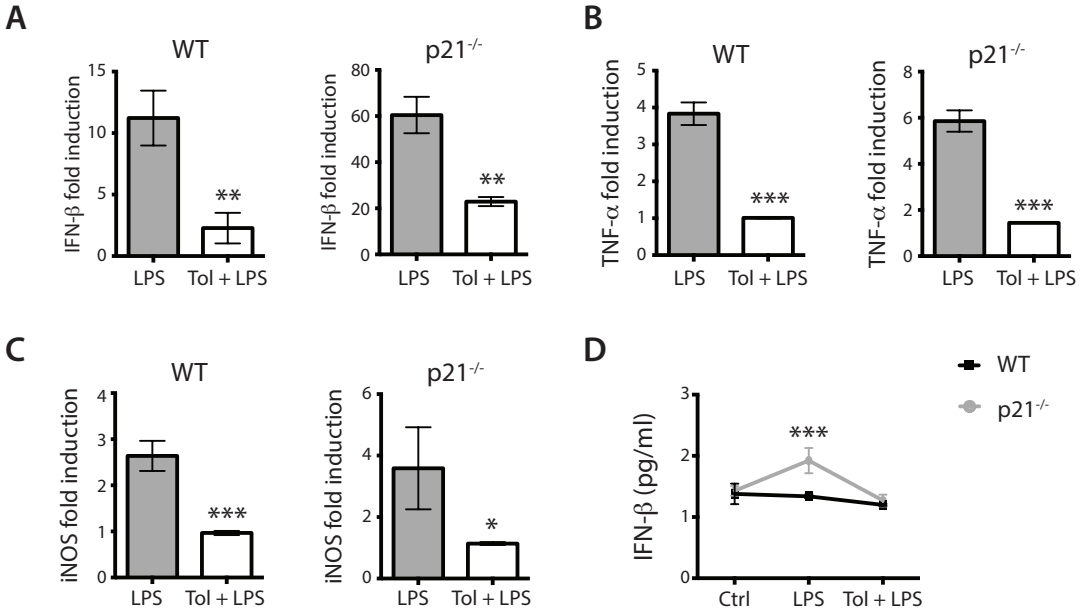

Figure S5. Lack of p21 increases LPS response in endothelial cells without affecting LPS-tolerance. Pulmonary endothelial cells were subjected to *in vitro* endotoxin tolerance (Figure 3). RT-PCR analysis showed reduced IFN-β (**A**), TNF-α (**B**) and iNOS (**C**) gene expression in LPS-tolerant WT and p21$^{-/-}$ cells. Results were normalized to β-actin and represent fold induction over WT unstimulated cells (not shown). (**D**) IFN-β protein levels in culture supernatants, as analyzed by ELISA. Data show mean ± SEM (n = 3 independent experiments), *p<0.05; **p<0.01; ***p<0.001, two-tailed Student's t test.

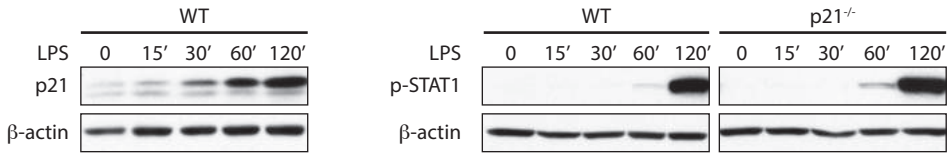

Figure S6. p21 and STAT1 phosphorylation levels after LPS activation. Immunoblot showing p21 and p-STAT1 protein levels in macrophage whole cell extracts after LPS activation at indicated times. β-actin is included as a loading control. Representative gels are shown of three experiments performed.

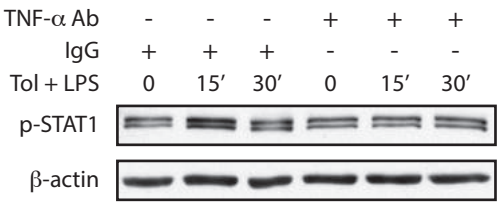

Figure S7. TNF-α neutralization does not affect STAT1 phosphorylation. p21$^{-/-}$ peritoneal macrophages were incubated with a TNF-α-neutralizing antibody or an isotype control during LPS tolerization (20 h). Cells were washed, cultured in medium (2 h) and restimulated with LPS (4 h). Immunoblotting showed similar STAT1 phosphorylation after antibody treatment at indicated times (Tol + LPS). A representative gel is shown of two experiments performed.

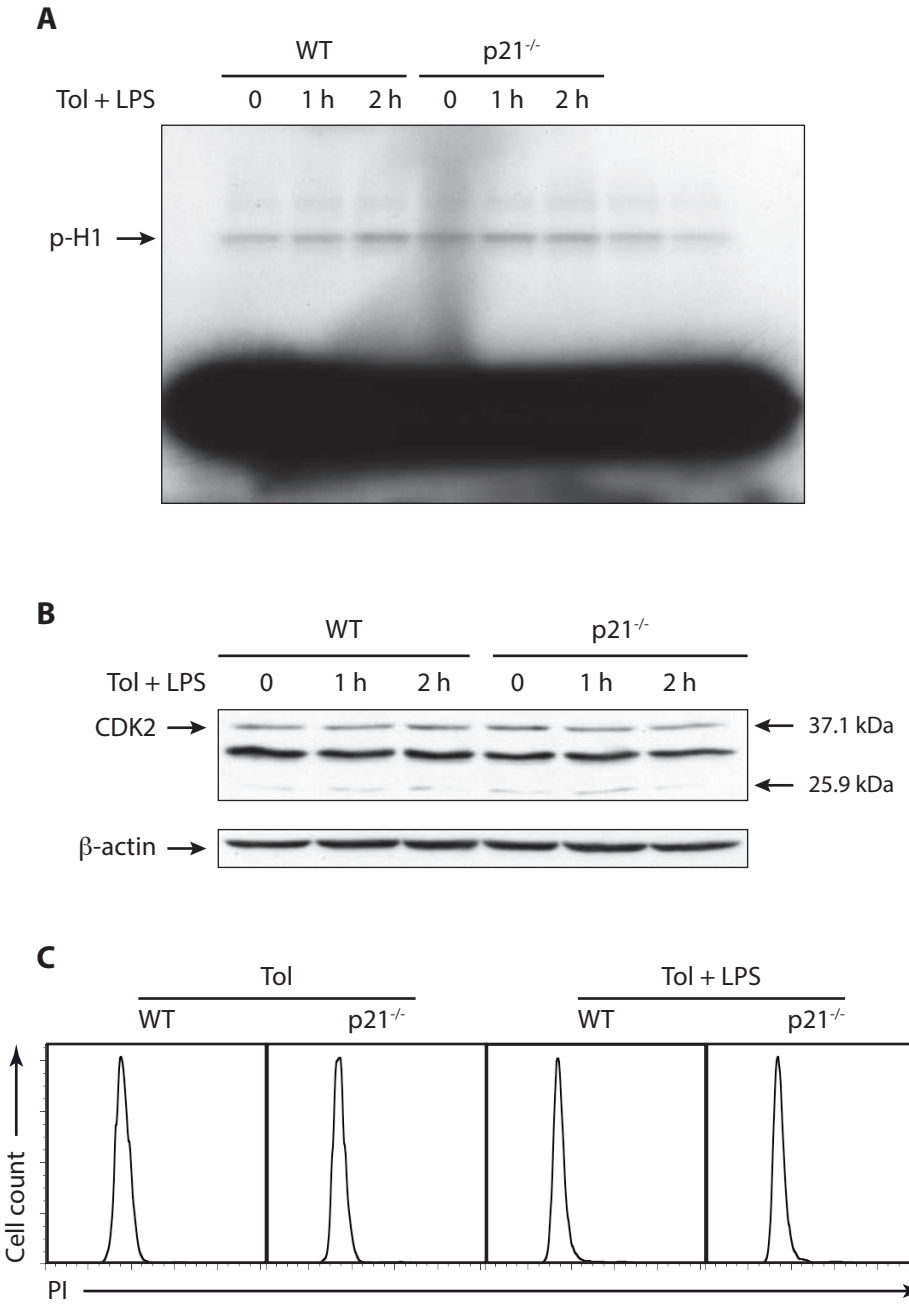

Figure S8. Impaired LPS tolerance in p21$^{-/-}$ macrophages is cell cycle-independent. (**A**) In WT and p21$^{-/-}$ LPS-tolerized macrophage extracts, CDK2 was immunoprecipitated and its kinase activity measured using histone H1 as a substrate. Assay products were resolved in SDS-PAGE, and phosphorylated H1 was detected by autoradiography. (**B**) Immunoblot showing CDK2 protein levels in LPS-tolerized peritoneal macrophages. Equal loading was confirmed by β-actin expression. (**C**) Cell cycle analysis by PI staining of LPS-tolerized and -restimulated macrophages. Representative results are shown of two independent experiments.

A

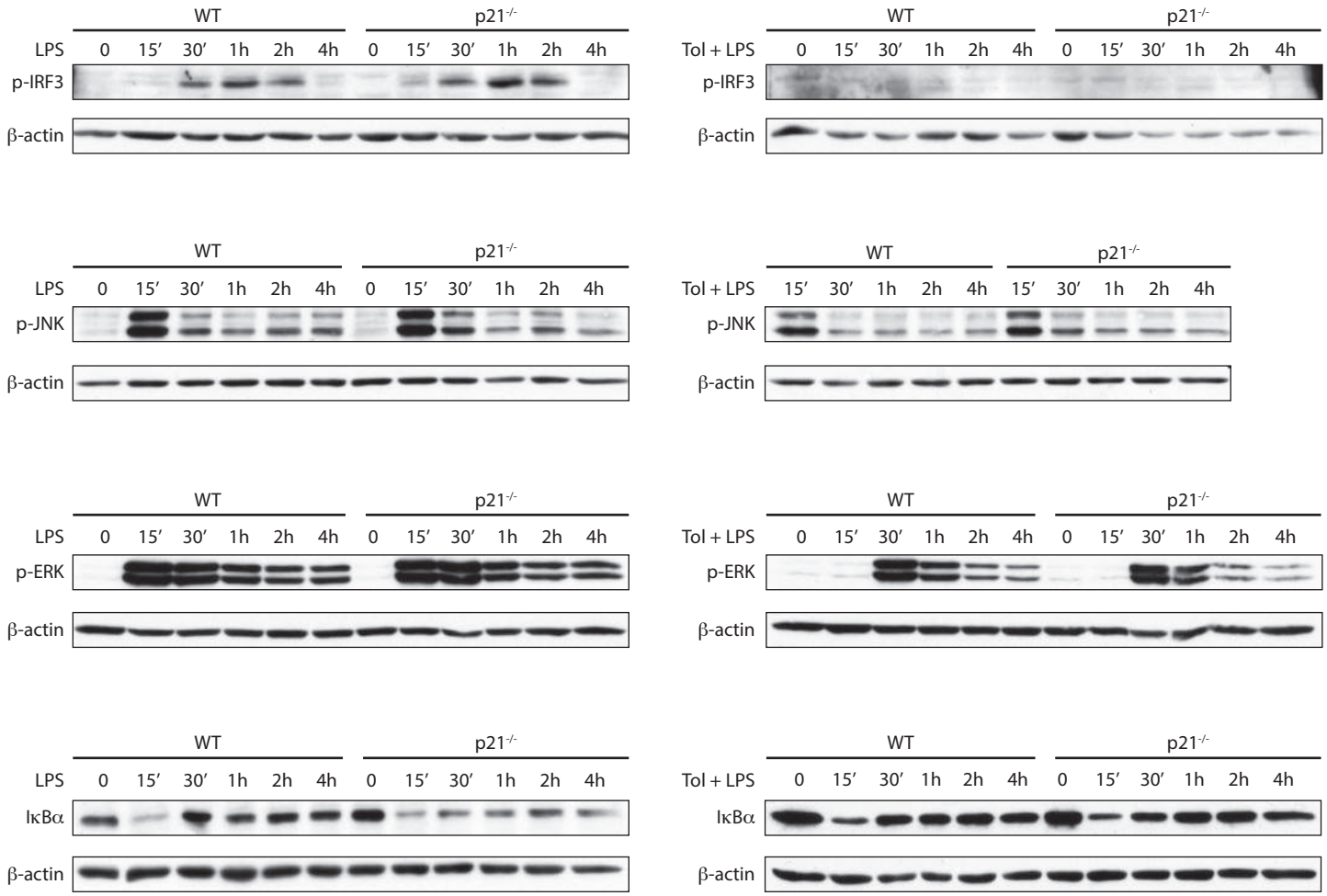

B

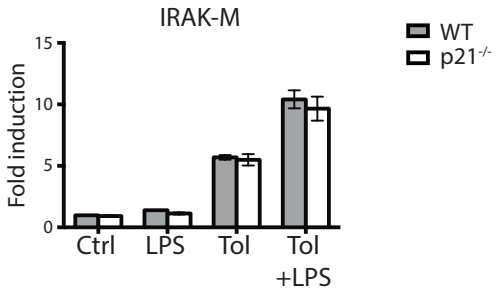

Figure S9. Lack of p21 does not affect IRF3, MAPK or NF-κB pathways in LPS-tolerized macrophages. (**A**) Immunoblots showing IRF3, ERK and JNK phosphorylation, and IκBα degradation at indicated times after LPS stimulation of resting or tolerized macrophages. β-actin is included as a loading control. Representative gels are shown of three experiments performed. (**B**) IRAK-M was induced at similar levels in LPS-tolerized WT and p21$^{-/-}$ macrophages. Results were normalized to β-actin and represent fold induction over unstimulated WT cells. Data shown as mean ± SEM (n = 3); ** p<0.01, two-tailed Student's t test.

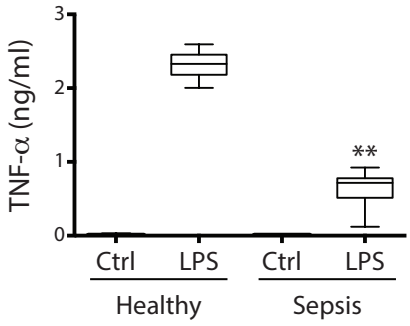

Figure S10. Hyporesponsiveness of sepsis monocytes. Monocytes isolated from sepsis patients are hyporesponsive to LPS (1 h) *in vitro* stimulation and show decreased TNF-*α* production compared with monocytes from healthy volunteers, as measured by cytometric bead array in culture supernatants. The median is shown ($n = 7$); $^{**}p<0.005$, two-tailed Mann-Whitney U test.

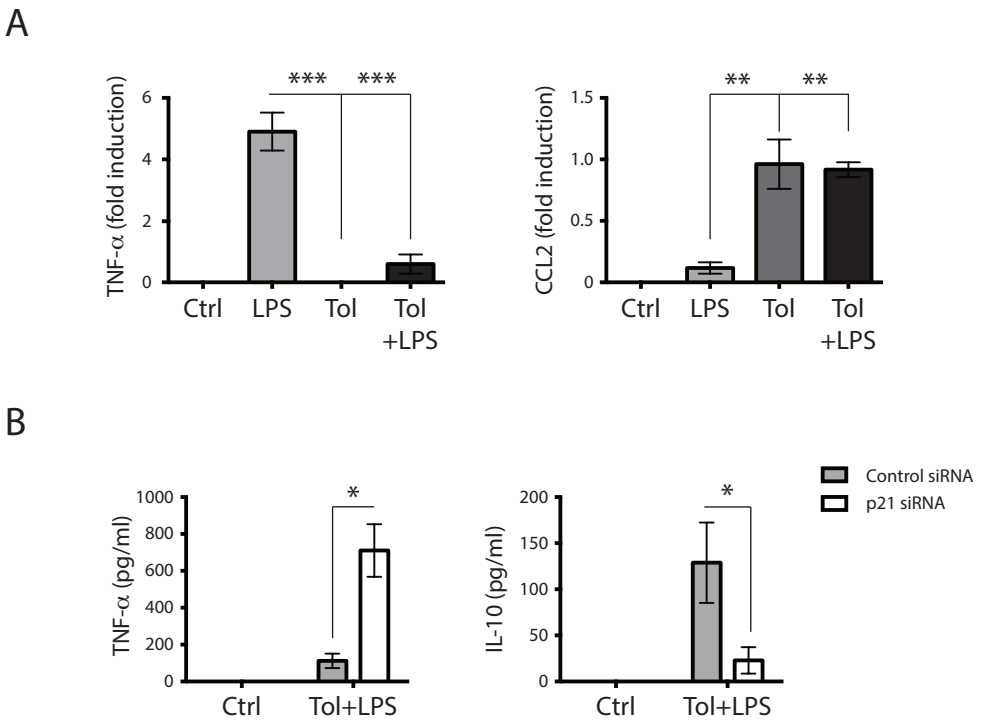

Figure S11. Effect of p21 on CCL2, TNF-α and IL-10 expression after LPS tolerization of human monocytes. (**A**) Human monocytes were isolated from healthy volunteers; resting or LPS-tolerized monocytes were then stimulated with LPS and analyzed by RT-PCR. LPS-tolerant human monocytes showed significant downregulation of TNF-α and upregulation of CCL2 expression compared with LPS-activated monocytes. Results were normalized to β-actin; (n = 4), one-way ANOVA. (**B**) Human monocytes were transfected with p21 or control siRNA and then LPS-tolerized and –rechallenged. Culture supernatants were analyzed for representative cytokine production by ELISA. In p21 siRNA-transfected tolerant human monocytes, TNF-α production was significantly increased while IL-10 production was decreased compared with control siRNA-transfected monocytes. Data shown as mean ± SEM (n = 3); *p<0.05; **p<0.01; ***p<0.001, two-tailed Student's t test.

Table I. Clinical parameters

	Data (n = 7)
Age	68 ± 10.6 years
Cardiac frequency	106.2 ± 3.9 pulsations/min
Respiratory frequency	24.1 ± 1.9 breaths/min
Temperature	38.4 ± 0.4 °C
Creatinine	2.4 ± 0.3 mg/dl
Hematocrit	36.1 ± 3.7
Leukocytes	18894.6 ± 3674.9 cells/mm^3
Neutrophils	15910 ± 3674.9 cells/mm^3
Glucose	134.7 ± 47.7 mg/dl
K^+	4.8 ± 0.6 mEq/L
Na^+	138.5 ± 2.7 mEq/L
CO_3H	17.6 ± 1.2 mmol/L
Glasgow-CS[A]	13.9 ± 0.86
SAPS	12 ± 1
Microbiology	Gram-negative bacteria

[A] Glasgow Coma Scale is a neurologic scale that aims to give a reliable and objective way to evaluate the neurologic damage in patients. Glasgow-CS is part of the APACHE II score. The normal value of Glasgow-CS is 15 (a healthy-normal parameter matched with age).
SAPS, simplified acute physiology score.